Equilibrium and Dynamical Properties of Hot and Dense Quark-Gluon matter from Holographic Black Holes

based on: Phys. Rev. D 104, 034002 & Phys. Rev. D 106, 034024

Joaquin Grefa

UNIVERSITY of HOUSTON

DEPARTMENT OF PHYSICS

with: Claudia Ratti & Israel Portillo(UH), Romulo Rougemont (UFG), Jacquelyn Noronha-Hostler, Jorge Noronha & Mauricio Hippert (UIUC), Raghav Kunnawalkam Elayavalli (VU)

XXXth International Conference on Ultra-relativistic Nucleus-Nucleus Collisions.
September 3 - 9

Outline

Table of Contents

QCD Phase Diagram

We can explore the QCD phase diagram by changing $\sqrt{s}$ in relativistic heavy ion collisions

Many models predict a first order phase transition line with a critical point

Lattice QCD is the most reliable theoretical tool to study the QCD phase diagram.

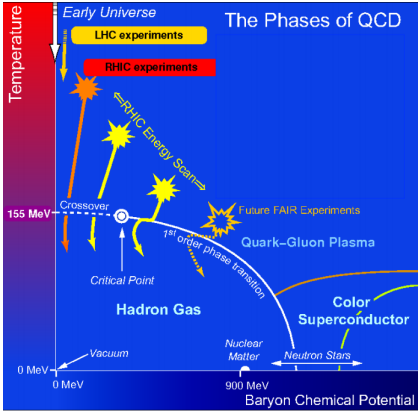

QCD Phase Diagram

We can explore the QCD phase diagram by changing $\sqrt{s}$ in relativistic heavy ion collisions

Many models predict a first order phase transition line with a critical point

Lattice QCD is the most reliable theoretical tool to study the QCD phase diagram.

Limitation

Sign problem

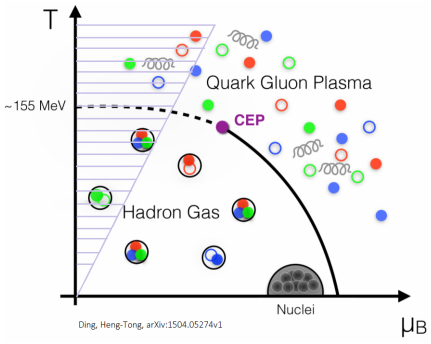

The model should exhibit:

-Deconfinement
-Nearly perfect fluidity
-Agreement with Lattice EoS at $\mu_B = 0$
-Agreement with baryon susceptibilities at $\mu_B = 0$

Taylor Expansion for small μ_B

$$\frac{P(T,\mu_B) - P(T,\mu_B = 0)}{T^4} = \sum_{n=1}^{\infty} \frac{1}{(2n)!} \chi_{2n}(T) \left(\frac{\mu_B}{T}\right)^{2n}$$

where $\chi_n(T,\mu_B) = \frac{\partial^n (P/T^4)}{\partial(\mu_B/T)^n}$

- How can we fulfill these conditions?

The model should exhibit:

-Deconfinement
-Nearly perfect fluidity
-Agreement with Lattice EoS at $\mu_B = 0$
-Agreement with baryon susceptibilities at $\mu_B = 0$

Taylor Expansion for small μ_B

$$\frac{P(T,\mu_B) - P(T,\mu_B = 0)}{T^4} = \sum_{n=1}^{\infty} \frac{1}{(2n)!} \chi_{2n}(T) \left(\frac{\mu_B}{T}\right)^{2n}$$

where $\chi_n(T,\mu_B) = \frac{\partial^n (P/T^4)}{\partial(\mu_B/T)^n}$

- How can we fulfill these conditions?

  HOLOGRAPHIC BLACK HOLES!!!

Table of Contents

Holographic gauge/gravity correspondence

5D Classical Gravity with asymptotically anti-de Sitter geometry	$\Longleftrightarrow$	3+1D Strongly coupled QFT in Minkowski spacetime

Maldacena 1997; Witten 1998; Gubser, Polyakov, Klebanov 1998

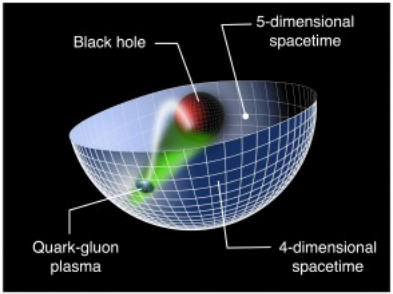

- Strongly coupled, nearly perfect fluid behavior of the QGP.
  Kovtun, Son, Starinets. PRL 94 (2005)

Holographic gauge/gravity correspondence

5D Classical Gravity with asymptotically anti-de Sitter geometry	$\Longleftrightarrow$	3+1D Strongly coupled QFT in Minkowski spacetime

Maldacena 1997; Witten 1998; Gubser, Polyakov, Klebanov 1998

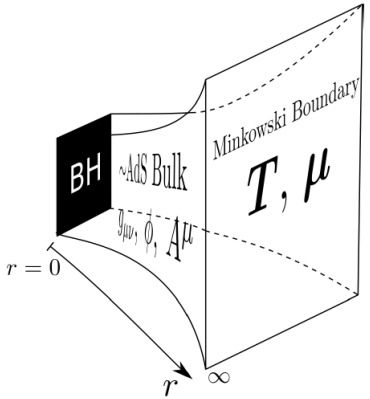

- Strongly coupled, nearly perfect fluid behavior of the QGP.
  Kovtun, Son, Starinets. PRL 94 (2005)
- BH solutions $\rightarrow$ QFT in T and μ.

Holographic gauge/gravity correspondence

5D Classical Gravity with asymptotically anti-de Sitter geometry	$\Longleftrightarrow$	3+1D Strongly coupled QFT in Minkowski spacetime

Maldacena 1997; Witten 1998; Gubser, Polyakov, Klebanov 1998

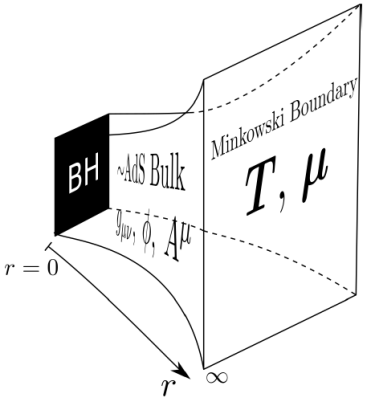

- Strongly coupled, nearly perfect fluid behavior of the QGP.
  Kovtun, Son, Starinets. PRL 94 (2005)
- BH solutions $\rightarrow$ QFT in T and μ.
- Can be constrained to mimic Lattice EoS at $\mu = 0$, and make predictions at finite density. J. G., et al. PRD 104 (2021) M. Hippert — Tuesday 9:50

Holographic gauge/gravity correspondence

5D Classical Gravity with asymptotically anti-de Sitter geometry	$\Longleftrightarrow$	3+1D Strongly coupled QFT in Minkowski spacetime

Maldacena 1997; Witten 1998; Gubser, Polyakov, Klebanov 1998

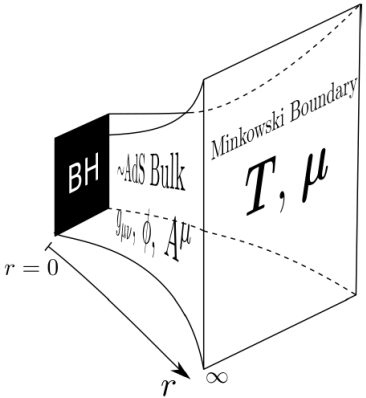

- Strongly coupled, nearly perfect fluid behavior of the QGP.
  Kovtun, Son, Starinets. PRL 94 (2005)
- BH solutions $\rightarrow$ QFT in T and μ.
- Can be constrained to mimic Lattice EoS at $\mu = 0$, and make predictions at finite density. J. G., et al. PRD 104 (2021) M. Hippert — Tuesday 9:50
- Able to handle near and out-of-equilibrium calculations.
  S. S. Gubser et al. PRL 101, (2008)
  J. G. et al. PRD 106 (2022)

Gravitational Action

O DeWolfe et al. Phys.Rev.D 83, (2011). R Rougemont et al. JHEP(2016)102. R. Critelli et al., Phys.Rev.D96(2017).

$$S = \frac{1}{2\kappa_5^2}\int_{M_5} d^5x\sqrt{-g}\left[R - \frac{(\partial_\mu\phi)^2}{2} - \underbrace{V(\phi)}_{\text{nonconformal}} - \underbrace{\frac{f(\phi)F_{\mu\nu}^2}{4}}_{\mu_B\neq 0}\right]$$

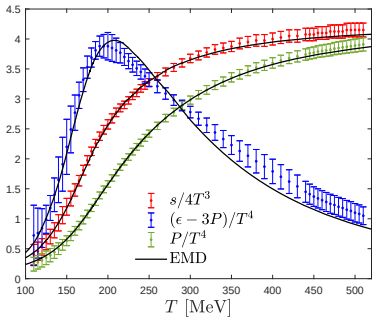

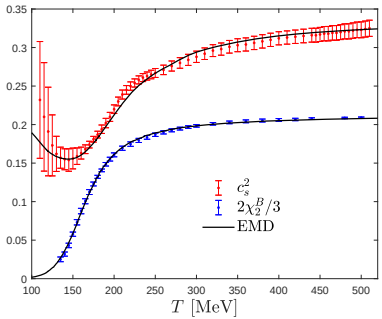

$$\chi_2(T,\mu_B) = \frac{\partial^2(P/T^4)}{\partial(\mu_B/T)^2} = \frac{\partial(\rho_B/T^3)}{\partial(\mu_B/T)}$$

Table of Contents

Locating the Critical End Point (CEP)

$T_{CEP} = 89$ MeV

$\mu_B^{CEP} = 724$ MeV

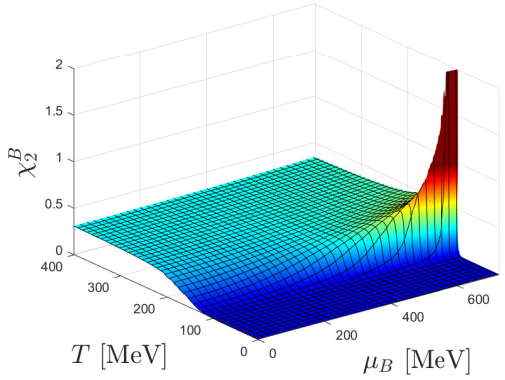

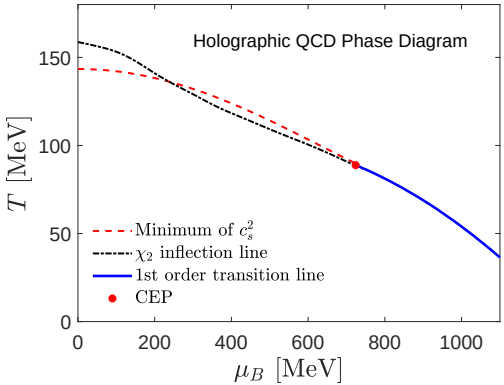

BH curves: J. G et al. PRD.104 (2021)

Comparison with the state-of-the-art lattice QCD thermodynamics

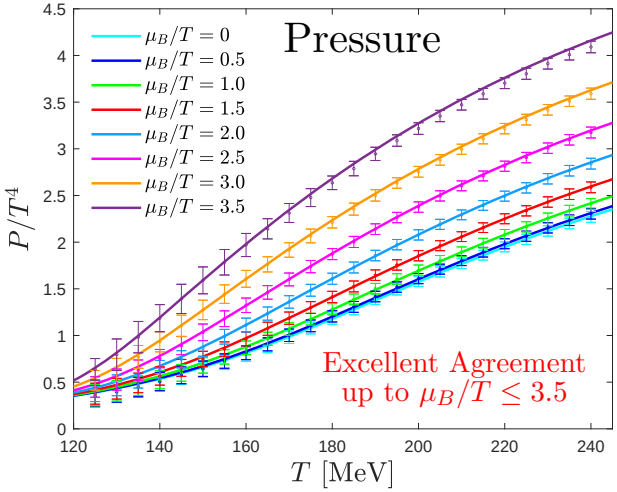

Lattice results: S. Borsanyi et al. 10.1103/PhysRevLett.126.232001

BH curves: J. G et al. PRD.104 (2021)

Comparison with the state-of-the-art lattice QCD thermodynamics

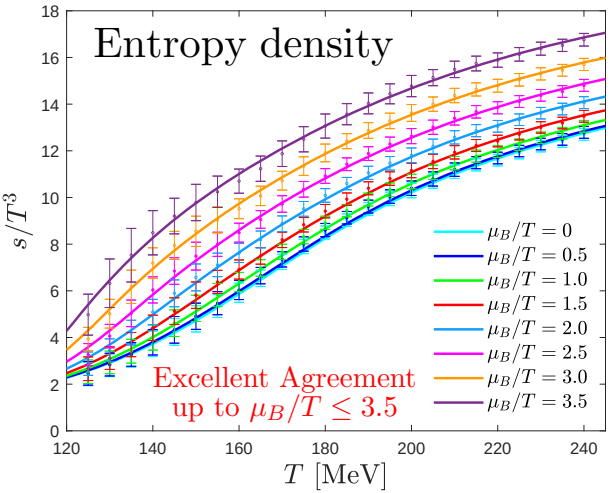

Lattice results: S. Borsanyi et al. 10.1103/PhysRevLett.126.232001

BH curves: J. G et al. PRD.104 (2021)

Equation of State

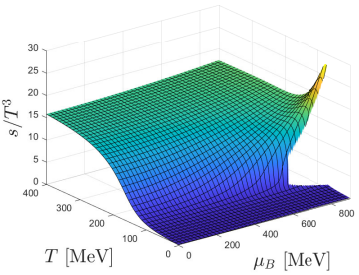

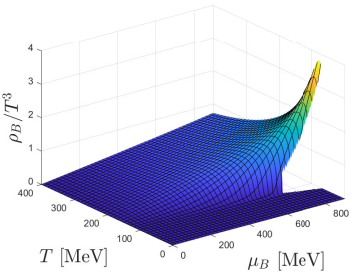

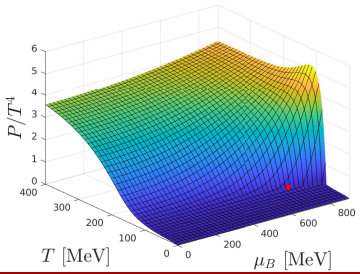

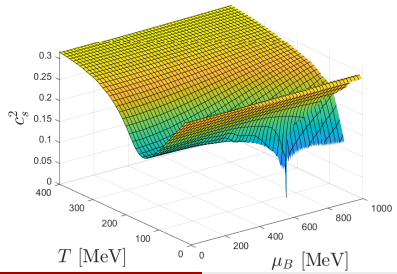

- Entropy density and baryon density exhibit a gap that corresponds to the line of first order phase transition.
- Critical point localized (see pressure)
- The minimum on c_2^2 corresponds to the location of the critical point.

plots: J. G et al. PRD.104 (2021)

Table of Contents

Baryon Conductivity σ_B

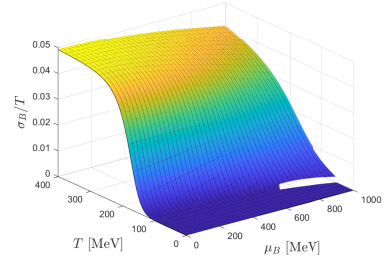

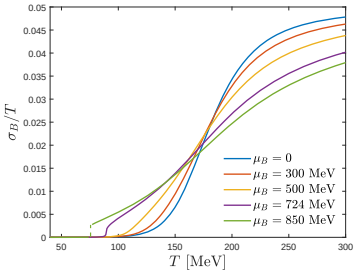

$$\sigma_B(T,\mu_B) = -\frac{\Lambda}{2\kappa_5^2\phi_A^{1/\nu}} \lim_{\omega\to 0} \frac{1}{\omega}\left(e^{2A} h f(\phi) \mathrm{Im}[a * a']\right) \text{ [MeV]}$$

Can be computed from linear perturbations to the black hole background fields.

Overall dependence of σ_B/T with μ_B is relatively small.

σ_B/T remains finite at the critical point, and exhibits a discontinuity over the line of first order phase transition.

plots: J.G. et al. PRD.106 (2022)

Baryon Diffusion Coefficient

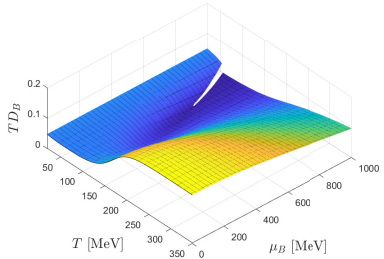

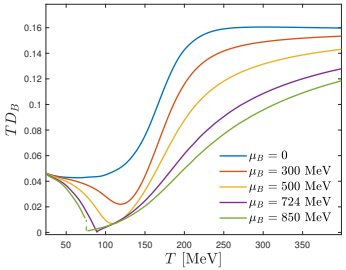

Nernst-Einstein Relation

$$D_B = \frac{\sigma_B}{\chi_2^B}$$

Controls the fluid response to inhomogeneities in the baryon density

The baryon diffusion charge is suppressed as the baryon chemical potential increases.

Vanishes at the location of the critical point.

plots: J.G. et al. PRD.106 (2022)

Holographic shear Viscosity

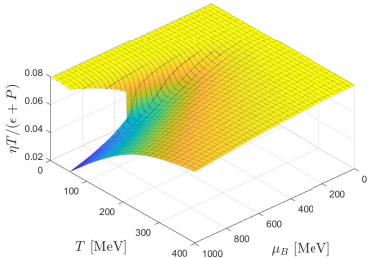

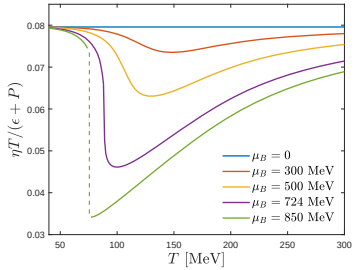

$$\frac{\eta}{s} = \frac{1}{4\pi}$$

$\eta T/(\epsilon + P)$

measures the resistance to deformation in the presence of a velocity gradient in the layers of the fluid.

$$\frac{\eta T}{\epsilon + P} = \frac{1}{4\pi}\frac{1}{1 + \frac{\mu_B \rho_B}{Ts}}$$

At $\mu_B = 0$, it reduces to the well known holographic result of $1/4\pi$

plots: J.G. et al. PRD.106 (2022)

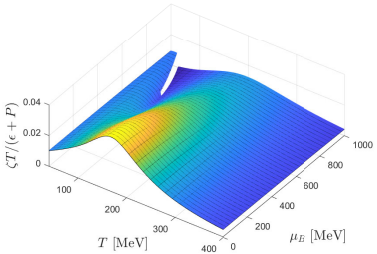

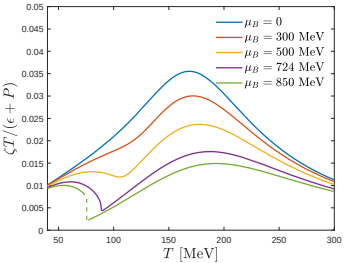

$$\frac{\zeta}{s} = -\frac{1}{36\pi}\lim_{\omega\to 0}\frac{1}{\omega}\left(\frac{e^{4A}h\phi'^2 Im[H^* H']}{A'^2}\right)$$

Measures the resistance to deformation of a fluid to a compression or expansion.

$$\frac{\zeta T}{\epsilon + p}(T, \mu_B) = \frac{\zeta}{s}\frac{1}{1 + \frac{\mu_B \rho_B}{Ts}}$$

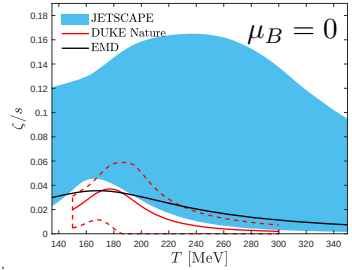

plots: J.G. et al. PRD.106 (2022)

Heavy quark Langevin Diffusion coefficient and jet quenching parameter

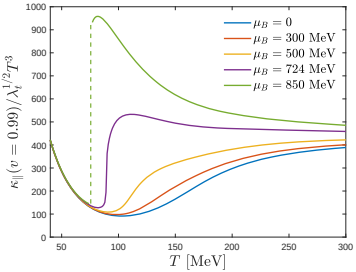

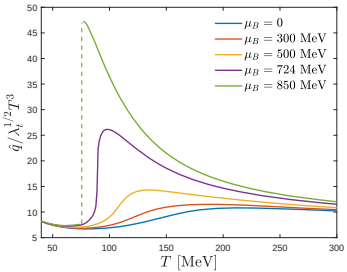

U. Gursoy et al. JHEP 0704 (2007)

Langevin diffusion coefficients

describe the thermal fluctuations of a heavy quark trajectory with constant velocity under Brownian motion.

F. D'Erano, H. Liu, K. Rajagopal. PRD 84 (2011)

The jet quenching parameter

characterizes the energy loss from collisional and radiative processes of high energy partons produced by the interaction with the hot and dense medium they travel through.

Their inflection point provides another way to characterize the crossover region.

plots: J.G. et al. PRD.106 (2022)

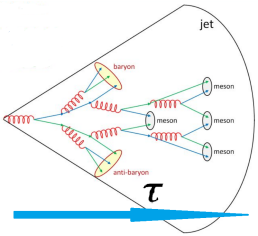

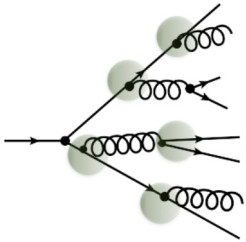

formation time

Time an emission takes to behave as an independent source of radiation.

$$\tau_{form} = \frac{1}{2Ez(1-z)(1-\cos\theta_{1,2})}$$

Energy and emission angle

taken from a distribution that depends on the jet quenching parameter $\hat{q}$

$$P(\theta,\omega) = \alpha\omega\theta^3\sqrt{\frac{2\omega}{\hat{q}}}L\exp\frac{-\theta^2\omega^2}{\sqrt{2\omega\hat{q}}}$$

L. Apolinario. Progress in Particle and Nuclear Physics, 103990

Translate T to τ

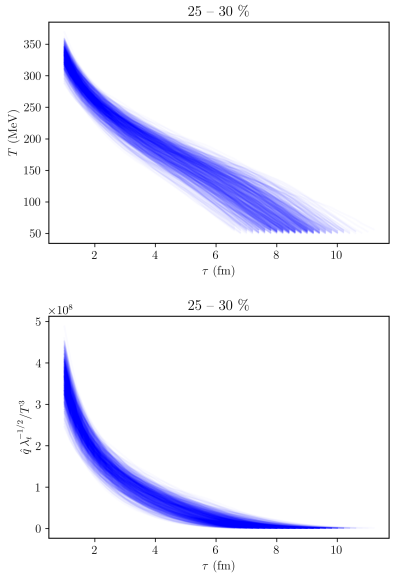

- TRENTo is used to model the initial state of relativistic heavy ion collisions.
- TRENTo provides a map of the energy density in the transverse plane (perpendicular to the collision axis) just after two heavy ions collide.
  Input: Holographic EoS.
- This energy density map is then evolved in time by using Bjorken hydrodynamics to model the QGP.

plots: J.G., Mauricio Hippert, et al (in preparation)

Translate T to τ

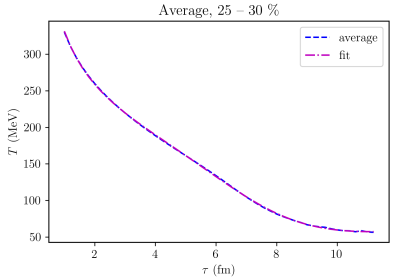

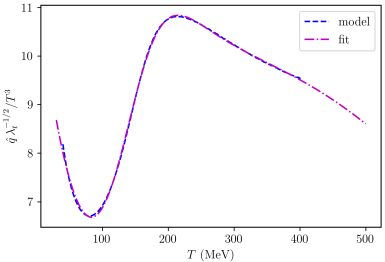

- TRENTo is used to model the initial state of relativistic heavy ion collisions.
- TRENTo provides a map of the energy density in the transverse plane (perpendicular to the collision axis) just after two heavy ions collide.
  Input: Holographic EoS.
- This energy density map is then evolved in time by using Bjorken hydrodynamics to model the QGP.
- The 't Hooft coupling (λ) should be fixed by phenomenological input.

plots: J.G., Mauricio Hippert, et al (in preparation)

Translate T to τ

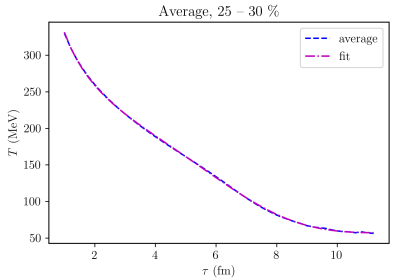

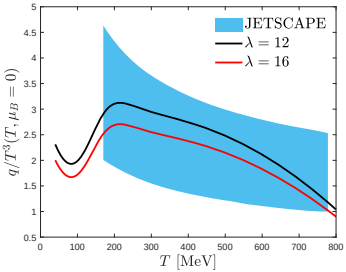

- T_RENTo is used to model the initial state of relativistic heavy ion collisions.
- T_RENTo provides a map of the energy density in the transverse plane (perpendicular to the collision axis) just after two heavy ions collide.
  Input: Holographic EoS.
- This energy density map is then evolved in time by using Bjorken hydrodynamics to model the QGP.
- The 't Hooft coupling (λ) should be fixed by phenomenological input.

plots: J.G., Mauricio Hippert, et al (in preparation)

JETSCAPE result taken from: L. Apolinario. Progress in Particle and Nuclear Physics, 103990

Preliminary results

Jets are less quenched as compared to a static $\hat{q}$. The overall degree of quenching of the jet population is reduced.

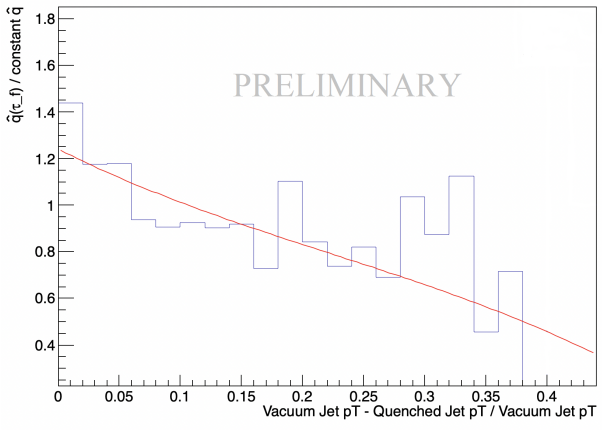

plots: J.G., Mauricio Hippert, et al (in preparation)

Table of Contents

Summary

- There is an excellent agreement between the Lattice QCD EoS and the Holographic result where there is lattice data available.
- The holographic model, which is fixed to mimic the Lattice EoS for $\mu_B = 0$, predicts a CEP. see M. Hippert — Tuesday 9:50
- With the first order phase transition line located in the QCD phase diagram, we considerably extended the baryon chemical potential coverage of the EoS in the QCD phase diagram.
- The transport coefficients related to transport of baryon charge, viscosities, and parton energy loss (12 in total) were obtained over finite baryon chemical potential, over the line of first order phase transition and the critical end point.
- The holographic transport coefficients can be potentially used to model jet energy loss.

Appendix

Thermodynamics at $\mu_B = 0$

Matching to Lattice EoS around the crossover

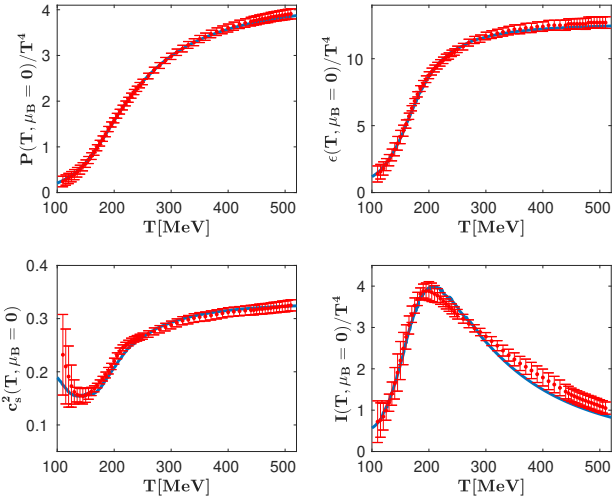

Mapping the QCD phase diagram from Black Hole solutions

The BH solutions are parametrized by (ϕ_0, Φ_1), where

$\phi_0 \rightarrow$ value of the scalar field at the horizon, and

$\Phi_1 \rightarrow$ electric field in the radial direction at the horizon

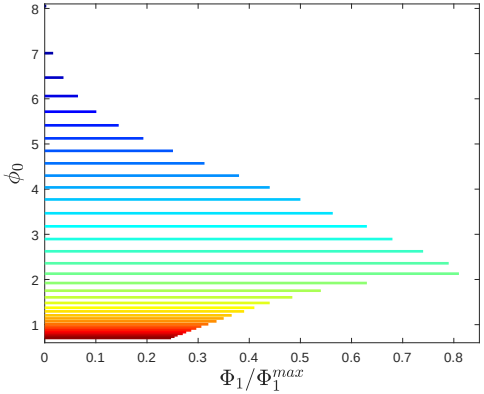

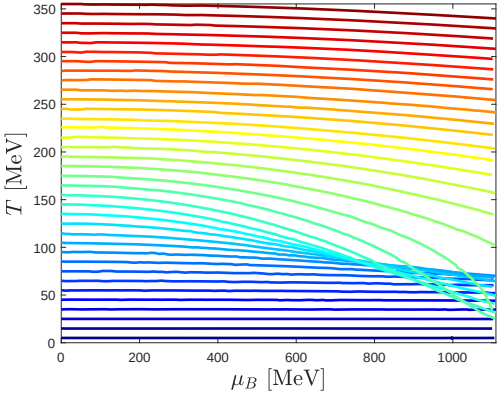

Locating the first order phase transition line

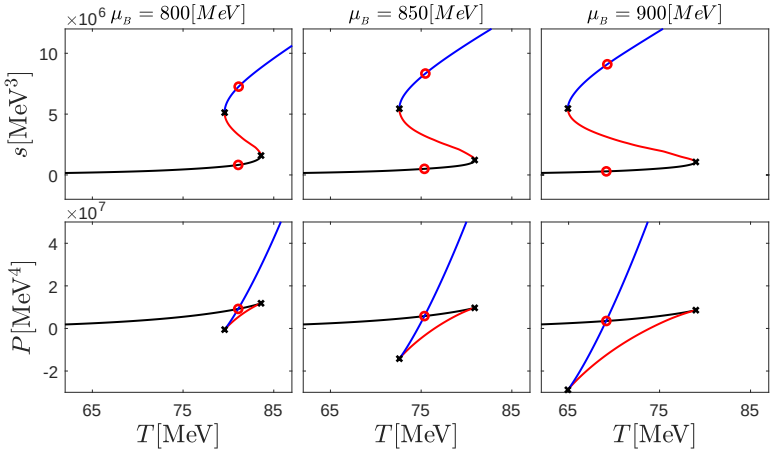

J. G et al. arXiv:2102.12042 [nucl-th].

$V(\phi)$ and $f(\phi)$

R. Critelli et al., Phys.Rev.D96(2017).
J. G et al. arXiv:2102.12042 [nucl-th].

Free Parameters for the Holographic Model

$$\kappa_5^2 = 8\pi G_5 = 8\pi(0.46), \qquad \Lambda = 1053.83 MeV,$$

$$V(\phi) = -12\cosh(0.63\phi) + 0.65\phi^2 - 0.05\phi^4 + 0.003\phi^6,$$

$$f(\phi) = \frac{\mathrm{sech}(c_1\phi + c_2\phi^2)}{1+c_3} + \frac{c_3}{1+c_3}\,\mathrm{sech}(c_4\phi),$$

where

$$c_1 = -0.27, \quad c_2 = 0.4, \quad c_3 = 1.7, \quad c_4 = 100$$

Equations of Motion

$$S = \frac{1}{2\kappa_5^2}\int_{M_5} d^5x\sqrt{-g}\left[R - \frac{(\partial_\mu\phi)^2}{2} - \underbrace{V(\phi)}_{\text{nonconformal}} - \underbrace{\frac{f(\phi)F_{\mu\nu}^2}{4}}_{\mu_B\neq 0}\right]$$

$$\begin{aligned} ds^2 &= e^{2A(r)}[-h(r)dt^2 + d\vec{x}^2] + \tfrac{e^{2B(r)}dr^2}{h(r)} \\ \phi &= \phi(r) \\ A_\mu dx^\mu &= \Phi(r)dt \end{aligned}$$

Equations of Motion

$$\phi''(r) + \left[\frac{h'(r)}{h(r)} + 4A'(r)\right]\phi'(r) - \frac{1}{h(r)}\left[\frac{\partial V(\phi)}{\partial\phi} - \frac{e^{-2A(r)}\Phi'(r)^2}{2}\frac{\partial f(\phi)}{\partial\phi}\right] = 0$$

$$\Phi''(r) + \left[2A'(r) + \frac{d[\ln f(\phi)]}{d\phi}\phi'(r)\right]\Phi'(r) = 0$$

$$A''(r) + \frac{\phi'(r)^2}{6} = 0$$

$$h''(r) + 4A'(r)h'(r) - e^{-2A(r)}f(\phi)\Phi'(r)^2 = 0$$

$$h(r)[24A'(r)^2 - \phi'(r)^2] + 6A'(r)h'(r) + 2V(\phi) + e^{-2A(r)}f(\phi)\Phi'(r)^2 = 0$$

Far-Region asymptotics:

$$A(r) = \alpha(r) + \mathcal{O}(e^{-2\nu\alpha(r)}), \qquad where\ \alpha(r) = A_{-1}^{far} r + A_0^{far}$$
$$h(r) = h_0^{far} + \mathcal{O}(e^{-4\alpha(r)}),$$
$$\phi(r) = \phi_A e^{-\nu\alpha(r)} + \mathcal{O}(e^{-(2+\nu)\alpha(r)}),$$
$$\Phi(r) = \Phi_0^{far} + \Phi_2^{far} e^{-1\alpha(r)} + \mathcal{O}(e^{-(2+\nu)\alpha(r)}),$$

Thermodynamics:

$$T = \frac{1}{4\pi\phi_A^{1/\nu}\sqrt{h_0^{far}}}\Lambda \qquad s = \frac{2\pi}{\kappa_5^2\phi_A^{3/\nu}}\Lambda^3$$

$$\mu_B = \frac{\Phi_0^{far}}{\phi_A^{1/\nu}\sqrt{h_0^{far}}}\Lambda \qquad \rho_B = -\frac{\Phi_2^{far}}{\kappa_5^2\phi_A^{3/\nu}\sqrt{h_0^{far}}}\Lambda^3$$

The EOM for the gauge invariant linearized vector perturbation $a(r,\omega)$ associated to the baryon conductivity is given by,

$$a'' + \left(2A' + \frac{h'}{h} + \frac{f'(\phi)}{f(\phi)}\phi'\right)a' + \frac{e^{-2A}}{h}\left(\frac{\omega^2}{h} - f(\phi)\Phi'^2\right)a = 0$$

which again must be solved with infalling wave condition at the horizon and normalized to unity at the boundary, what may be done by setting,

$$a(r,\omega) = \frac{r^{-i\omega}P(r,\omega)}{r_{max}^{-i\omega}P(r_{max},\omega)}$$

The DC baryon conductivity in the EMD model is calculated by means of the following holographic Kubo formula,

$$\sigma_B(T,\mu_B) = -\frac{\Lambda}{2\kappa_5^2\phi_A^{1/\nu}}\lim_{\omega\to 0}\frac{1}{\omega}\left(e^{2A}hf(\phi)Im[a*a']\right)[MeV]$$

Bulk Viscosity

The equation of motion (EOM) for the gauge and diffeomorphism invariant linearized scalar perturbation $H(r,\omega)$ associated to the bulk viscosity through the holographic dictionary is,

$$H'' + \left(4A' + \frac{h'}{h} + \frac{2\phi''}{\phi} - \frac{2A''}{A'}\right) H' +$$

$$\left[\frac{e^{-2A}\omega^2}{h^2} + \frac{h'}{h}\left(\frac{A''}{A'} - \frac{\phi''}{\phi'}\right) + \frac{e^{-2A}}{h\phi'}(3A'f'(\phi) - f(\phi)\phi')\Phi'^2\right] H = 0$$

which must be solved with infalling wave condition at the black hole horizon, and normalized to unity at the boundary, what may be done be setting,

$$H(r,\omega) = \frac{r^{-i\omega}F(r,\omega)}{r_{max}^{-i\omega}F(r_{max},\omega)}$$

The ratio between the bulk viscosity and the entropy density in the EMD model is then calculated by making use of the following holographic Kubo formula,

$$\frac{\zeta}{s}(T,\mu_B) = -\frac{1}{36\pi}\lim_{\omega\to 0}\frac{1}{\omega}\left(\frac{e^{4A}h\phi'^2 Im[H^*H']}{A'^2}\right)$$

Transport coefficients Formulas

$$\frac{F_{\rm drag}}{\sqrt{\lambda_t}T^2}(T,\mu_B;v) = -8\pi v h_0^{\rm far} e^{\sqrt{2/3}\phi(r_*)+2A(r_*)},$$

$$h(r_*) = h_0^{\rm far} v^2$$

$$\frac{\kappa_\parallel}{\sqrt{\lambda_t}T^3}(T,\mu_B;v) = 16\pi v^3 (h_0^{\rm far})^{5/2} \frac{e^{\sqrt{2/3}\phi(r_*)+3A(r_*)}}{h'(r_*)^2} \times$$
$$\times \left(h'(r_*)\left[4A'(r_*) + \sqrt{\frac{8}{3}}\phi'(r_*) + \frac{h'(r_*)}{h(r_*)}\right]\right)^{3/2},$$

$$\frac{\hat{q}}{\sqrt{\lambda_t}T^3}(T,\mu_B) = \frac{64\pi^2 h_0^{\rm far}}{\int_{r_{\rm start}}^{r_{\rm max}} dr \frac{e^{-\sqrt{2/3}\phi(r)-3A(r)}}{\sqrt{h(r)\left[h_0^{far}-h(r)\right]}}}$$

Collision Energy Estimates

We estimate a collision energy needed to hit the CEP

- $\sqrt{s} = 2.5 - 4.1$ GeV

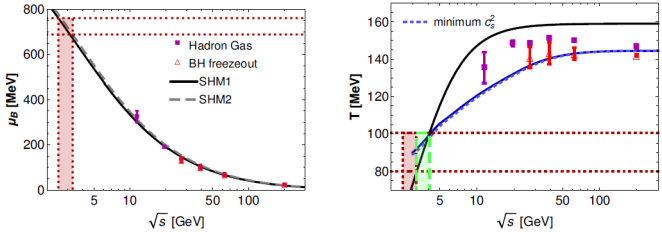

- The collision energy is reachable by the next generation of experiments.

[BH] R.Critelli, I.P. et al., Phys.Rev.D**96**(2017).
[HRG] Paolo Alba et al. Phys.Lett.B**738**(2014),
[SHM1] A. Andronic et al. Phys.Lett.B**673**(2009).
[SHM2] J. Cleymans et al. Phys.Rev.C**73**(2006).

The QCD Critical Point

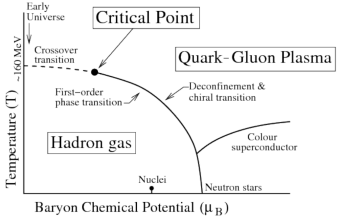

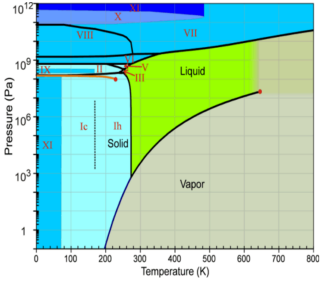

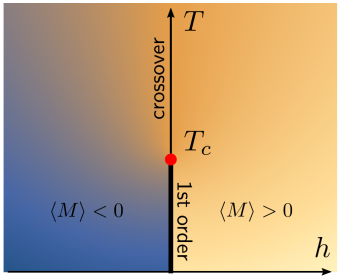

Low T EoS

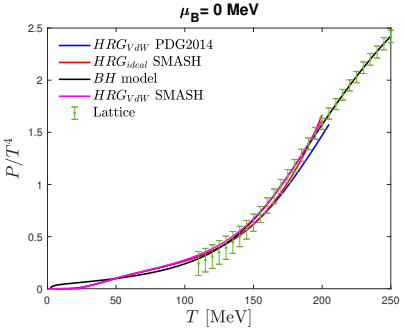
μ_B= 0 MeV
HRG_{VdW} PDG2014
HRG_{ideal} SMASH
BH model
HRG_{VdW} SMASH
Lattice
P/T^4
T [MeV]
0
0.5
1
1.5
2
2.5
0
50
100
150
200
250

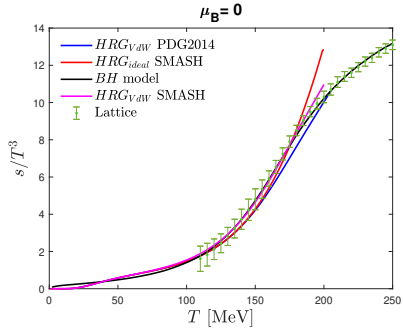
μ_B= 0
HRG_{VdW} PDG2014
HRG_{ideal} SMASH
BH model
HRG_{VdW} SMASH
Lattice
s/T^3
T [MeV]
0
2
4
6
8
10
12
14
0
50
100
150
200
250

- Susceptibilities $\chi_n^B = \frac{\partial^n (P/T^4)}{\partial (\mu_B/T)^n}$
- Susceptibilities χ_n^B are directly related to the moments of the distribution
- Volume independent ratios are useful to compare experimental data

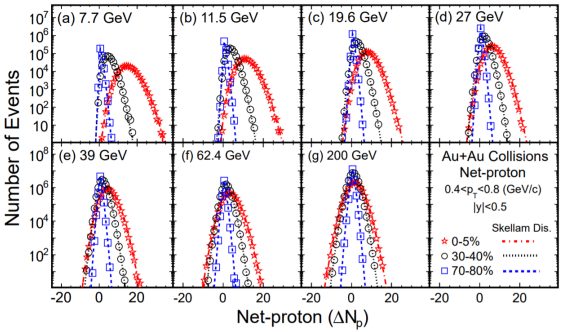

L. Adamczyk et al. Phys. Rev. Lett. 112 (2014), p. 032302.

mean: $M \sim \chi_1$

variance: $\sigma^2 \sim \chi_2$

skewness: $S \sim \chi_3/\chi_2^{3/2}$

kurtosis: $\kappa \sim \chi_4/\chi_2^2$

$$M/\sigma^2 = \chi_1/\chi_2$$
$$S\sigma = \chi_3/\chi_2$$
$$\kappa\sigma^2 = \chi_4/\chi_2$$
$$S\sigma^3/M = \chi_3/\chi_1$$

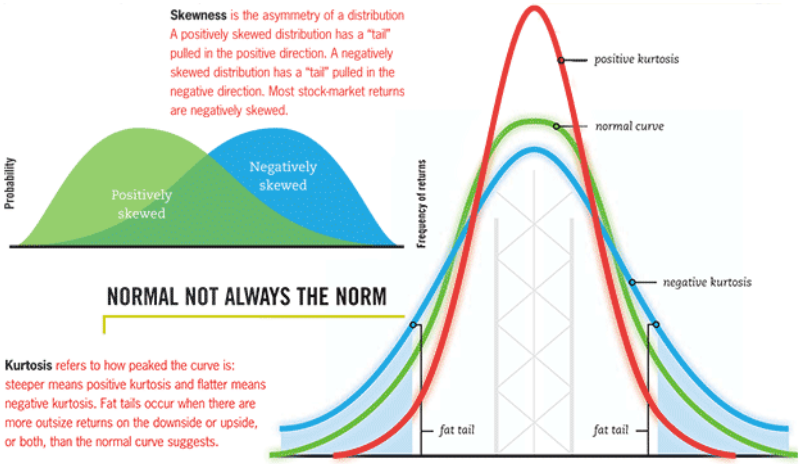
Skewness is the asymmetry of a distribution
A positively skewed distribution has a "tail" pulled in the positive direction. A negatively skewed distribution has a "tail" pulled in the negative direction. Most stock-market returns are negatively skewed.
Probability
Positively skewed
Negatively skewed
NORMAL NOT ALWAYS THE NORM
Kurtosis refers to how peaked the curve is: steeper means positive kurtosis and flatter means negative kurtosis. Fat tails occur when there are more outsize returns on the downside or upside, or both, than the normal curve suggests.
Frequency of returns
positive kurtosis
normal curve
negative kurtosis
fat tail
fat tail

Higher Order Baryon Susceptibilities

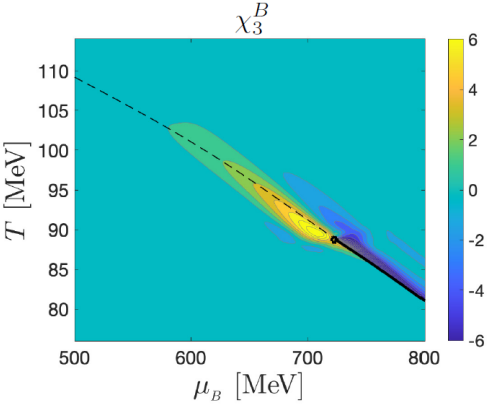

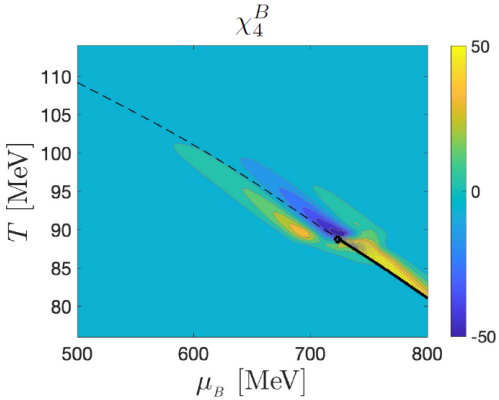

Multidimensional QCD phase diagram

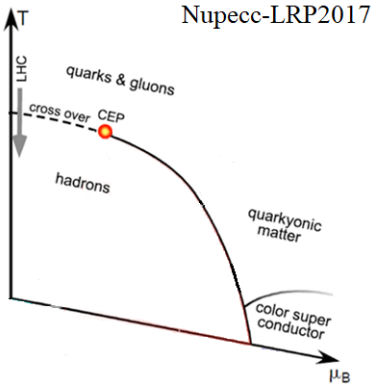

Multidimensional QCD phase diagram

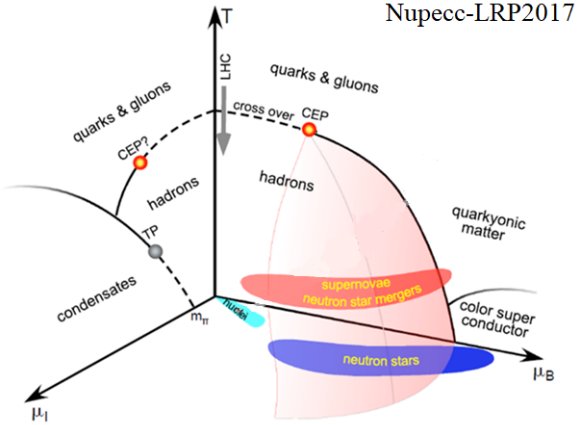

Multidimensional QCD phase diagram

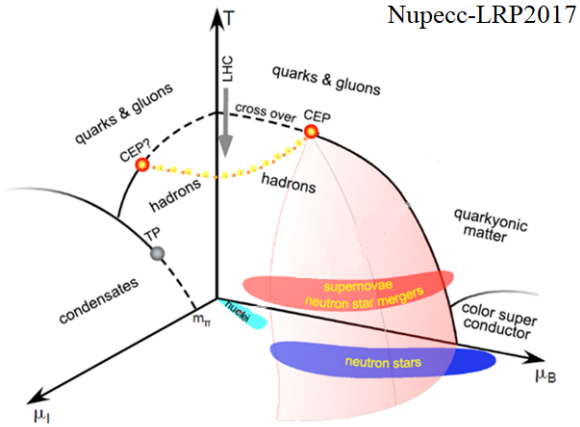

Strangeness Susceptibility Matching